Effect of trace impurities in perchloric acid on blank voltammetry of Pt(111)

Fröhlich, N.; Fernández Vidal, J.; Mascaró, F.V.; Shih, A. J.; Luo, M.; Koper, M.T.M.

Electrochimica Acta 466 (2023) 143035

Contents lists available at ScienceDirect

Electrochimica Acta

journal homepage: www.journals.elsevier.com/electrochimica-acta

Effect of trace impurities in perchloric acid on blank voltammetry of Pt (111)

Nicci Fröhlich [a,1], Julia Fernández-Vidal [a,1], Francesc Valls Mascaró [a], Arthur J. Shih [a,b], Mingchuan Luo [a,c], Marc T.M. Koper [a,*]

[a] Leiden Institute of Chemistry, Leiden University, Einsteinweg 55, 2333 CC Leiden, the Netherlands
[b] Department of Materials Science and Engineering, Northwestern University, Evanston, IL 60208, USA
[c] School of Materials Science and Engineering, Peking University, Beijing 100871, China

ARTICLE INFO

Keywords:
Pt(111)
Blank voltammetry
Impurities
Perchloric acid

ABSTRACT

Trace impurities of nitrate and sulphate species have been detected as the cause for the charge quench of existing voltammetric peaks and the appearance of new voltammetric peaks in the blank voltammetry of Pt(111) in high-purity perchloric acid. Cyclic voltammetry of Pt(111) in high concentrations of $HClO_4$ (1 M) electrolyte display anomalous reduction peaks at 0.5 and 0.32 V_{RHE}. The reduction of nitrates to nitric oxide, resulting in the reduction peak at 0.32 V_{RHE}, has been detected using *in situ* Fourier transform infrared spectroscopy. The peak at 0.5 V_{RHE}, previously assigned in the literature to specific adsorption of perchlorate anions catalytically dissociating to chloride anions, is consistent with sulphate desorption as elucidated by spiking $HClO_4$ electrolyte with trace quantities (10 ppm) of sulphuric acid. The presence of kosmotropic sulphate anions was further confirmed by the positive onset potential shift of the sharp OH_{ads} butterfly peak at ~0.8 V_{RHE} with increasing concentrations of $HClO_4$ (0.01–1 M). Although commonly overlooked, we show here the marked deleterious impact these trace impurities have on the blank voltammetry of Pt(111), and provide recommendations for minimising this impact.

1. Introduction

Fundamental electrochemical studies on single-crystalline surfaces have great interest in electrochemistry as their surface structure is closely controlled on an atomic level and, therefore, they present an ideal system to study surface-sensitive reactions [1–5]. The cyclic voltammograms (CVs) of single crystal electrodes display features characteristic for each of the facets, varying as a function of the width of the terraces and the density and type of steps/defects on the single crystal surface [6]. Hence, cyclic voltammetry is often highly sensitive to both the local nanoscopic surface morphology of the single crystal surface and the surface density of adsorption sites and/or nature of adsorbed species from the electrolyte via the relative intensities of the corresponding voltammetric peaks. Any adsorption of electroactive species results in such a voltametric peak, where an increase in peak broadness reveals repulsive interactions between adsorbates [7]. The voltammogram of a particular single crystal surface then effectively becomes a characteristic fingerprint of the crystallographic structure, in a given electrolyte. Changes or irregularities in these profiles suggest a lack of surface order, changes in adsorbed species, the electrical double layer, and/or the possible presence of impurities. Hence, electrolyte cleanliness would impact specific adsorption and thus change the voltammetric response [8].

Perchloric acid is commonly used to characterise the surface of single crystals such as Au and Pt as, in principle, no specific adsorption of perchlorate anions occurs [9]. The only electrosorption that is assumed to occur in $HClO_4$ electrolyte is that of hydrogen and hydroxide species ($H_{ads/des}$, $OH_{ads/des}$) from H_2O dissociation [10–16]. However, even with the establishment of Clavilier's flame-annealing method for Pt single crystal surface preparation in 1980 [2,17], electrolyte cleanliness remains a significant concern, even in the highest purity electrolyte solutions commercially available. The presence of impurities can affect the voltammetric response in very subtle ways [18,19].

Pt(111) is the most compact Pt basal plane, is highly stable, and has a very characteristic voltammetric response. Firstly described by Clavilier [2,17], the CV of Pt(111) in $HClO_4$ has been well-established in the

* Corresponding author.
E-mail address: m.koper@chem.leidenuniv.nl (M.T.M. Koper).
[1] These authors contributed equally.

https://doi.org/10.1016/j.electacta.2023.143035
Received 30 June 2023; Received in revised form 26 July 2023; Accepted 16 August 2023
Available online 18 August 2023

literature, with clearly defined regions: hydrogen under-potential deposition, H_{upd} (0.05–0.4 V *vs.* RHE); double-layer region (0.4–0.55 V); and hydroxyl adsorption, OH_{ads} (0.55–0.85 V) [20]. Pt(111) single crystals are seldom devoid of defects, such that small voltammetric peaks are often visible at ~0.13 V and ~0.28 V, attributed to the co-adsorption of hydrogen and hydroxyl species at (110) and (100) defect sites, respectively [21,22].

The voltammetric feature in the OH_{ads} region, also known as the "butterfly" peak, is comprised of two regions: (i) a broad increase in voltammetric current similar to that of the H_{upd}; and (ii) a sharp peak at ~0.8 V. The origin of the shape of the butterfly feature remains a source of debate in the literature. A number of groups argue that this sharp peak is related to a reorganisation of the OH_{ads} compact adlayer structure in terms of an order–disorder phase transition [23–26], while Feliu et al [5] attribute these two regions to the adsorption of two respective types of water forming OH_{ads} in the process. Regardless, the sharpness of the voltammetric features and the symmetry of the reversible adsorption states on Pt, *i.e.*, H and/or OH adsorption/desorption processes, can be used as a proxy for surface and electrolyte cleanliness as specific adsorption and defects cause a concurrent decrease in the peak current density of the sharp peak [27–30]. Changes in the onset potential of the sharp peak at ~0.8 V have also been attributed to the presence of different types of anions in the electrolyte [5,31], which, in turn, change the local water structure by enhancing/inhibiting hydrogen bonding respectively, creating two classes of anion: (i) kosmotropic (structure ordering) anions such as sulphates, which cause a shift to more positive onset potentials, and (ii) chaotropic (structure breaking) anions such as chloride, which result in a shift to more negative onset potentials [5, 32–34].

In the past, work by Watanabe et al [35,36] and Attard et al [31] have discussed the possibility of specific adsorption of ClO_4^- anions on Pt {*hkl*} single crystal electrodes from $HClO_4$ using a combination of cyclic voltammetry, quartz crystal microbalance and *in situ* infra-red spectroscopy studies. Due to competitive adsorption for sites on Pt with Cl^- anions produced from the slow catalytic dissociation of specifically adsorbed ClO_4^- anions, the adsorption of H and OH species becomes inhibited, where the inhibition of adsorption of OH species, in particular, has been shown to reduce the efficiency of the oxygen reduction reaction (ORR) by an order of magnitude [19,37–40].

However, an often-overlooked aspect of perchloric acid is the presence of trace impurities, particularly that of nitrates and sulphates at 3–10 ppm concentrations in some of the highest-grade purity $HClO_4$ solutions available (60/70% Merck Suprapur®). The groups of Markovic [41] and Kocha [19] have previously highlighted the extreme sensitivity of ORR activity to trace levels of nitrates and chlorides. The effect of low concentrations of nitrate on the CV of Pt(110) was further elucidated in a patent released by Strmcnik et al [42], where a purification method for the removal of trace level impurities down to a concentration of 10^{-8}M was detailed. They showed that after purification, no detectable quenching of the charge density was observed in the CV of Pt(110) in 10^{-5}M $HClO_4$. However, the question of whether this same purification method would remain as effective and efficient for higher concentration $HClO_4$ solutions remains.

In this manuscript, we show that the non-negligible presence of these trace impurities, coupled with their high affinity for Pt, contribute to site-blocking effects, which, in turn, result in marked perturbations across the CV of Pt(111). In this sense, we thereby highlight the importance of considering the presence of impurities when carrying out experiment in this electrolyte, and by extension when studying any single crystal surface [19,43,44]. We will also elucidate and illustrate under which conditions these trace impurities can so significantly change the Pt(111) CV that the results may be easily misinterpreted. We believe that these conditions could be especially relevant for certain long-term *in situ* spectroscopic experiments carried out on Pt(111) (or, by extension, other Pt surfaces).

2. *Experimental*

2.1. *Electrochemical*

All glassware was placed in a mixture of H_2SO_4 and $KMnO_4$ at pH 1 overnight and rinsed with a diluted mixture of H_2SO_4 and H_2O_2 at 10% in ultra-high purity water (Milli-Q, 18.2 MΩ cm) followed by repetitive rinsing and boiling with ultra-high purity water. Cyclic voltammetry measurements were carried out using a standard three-electrode cell assembly with a parallel shunt capacitor to the reference electrode at 23 °C and a Bio-Logic VSP300 potentiostat. A Pt(111) disc-type electrode of 3.0 mm diameter purchased from MaTeck (99.999%) was used as the working electrode. A homemade reversible hydrogen electrode (RHE) was used as the reference electrode and Pt wires were used as the counter and additional shunt capacitor of 10 μF (connected with the RHE). All the potentials in this manuscript are reported *versus* the RHE scale. Pt(111) single-crystal electrode was prepared following the method reported by Clavilier [2,17]; flame annealed with a butane torch and then immediately brought into contact with an Ar:H_2 (1:1) environment in order to obtain a well-ordered 111 structure. Once cooled to room temperature, the crystal surface was quenched with a Ar/H_2-saturated drop of ultra-high purity water to avoid oxidation of the surface when transferred to the electrochemical cell. The Pt(111) single-crystal was brought into the hanging meniscus configuration under a controlled potential of 0.07 V. The quality of the crystal and cleanliness of the cell were checked by recording a blank voltammogram of the Pt(111) crystal in the chosen concentration of $HClO_4$ electrolyte (60% Merck Suprapur®) purged with Ar gas (Linde 5.0, ≥99.999%) through polytetrafluoroethylene (PTFE) gas tubing preventing O_2 permeation. The gas tubing was also regularly cleaned to prevent contamination using the same procedure detailed for the glassware above. Throughout the measurements, a constant Ar gas blanket above the electrolyte was maintained to prevent O_2 from entering the cell. $NaClO_4.H_2O$ (≥ 99% Merck EMSURE®) was used for salt additions.

2.2. *FTIR*

In situ FTIR spectra were collected using a Bruker Vertex 80 V IR spectrometer equipped with a liquid nitrogen cooled MCT detector. Background spectrum was recorded before each spectral series at 0.50 V. This potential was chosen to minimise changes in the baseline of the spectra as it is included in the double layer region where, in principle, no specific adsorption is occurring.

The collected spectra are presented in absorbence units (a.u.), according to $-\log(R/R_0)$, where R corresponds to the reflectance of the sample and R_0 to the reflectance of the background spectrum. The positive bands in the spectra correspond to the adsorption of species that were either absent or at lower concentrations at 0.50 V, while the negative bands in the spectra correspond to the desorption of species present at said potential.

FTIR spectra were obtained between 2000–1000 cm^{-1} by accumulating 100 interferograms per spectrum with a spectral resolution of 2 cm^{-1} in a three-electrode spectro-electrochemical cell with an IR-transparent CaF_2 prism attached to the bottom of the cell. Details of the *in situ* FTIR cell have been given elsewhere [45].

3. *Results and discussion*

In order to study the effect of $HClO_4$ concentration on Pt(111), the CVs in 0.01, 0.1 and 1 M $HClO_4$ electrolyte have been recorded (Fig. 1). Three well-defined regions: H_{upd} (0.07–0.4 V), double-layer (0.4–0.55 V) and OH_{ads} (0.55–0.85 V), can be observed in the blank CVs of 0.01 and 0.1 M $HClO_4$, consistent with that of a clean Pt(111) surface reported in the literature [20]. However, we observe a decrease in the charge density of the OH_{ads} butterfly peak (0.55–0.85 V) at increased $HClO_4$ concentrations, as well as a non-Nernstian shift to more positive

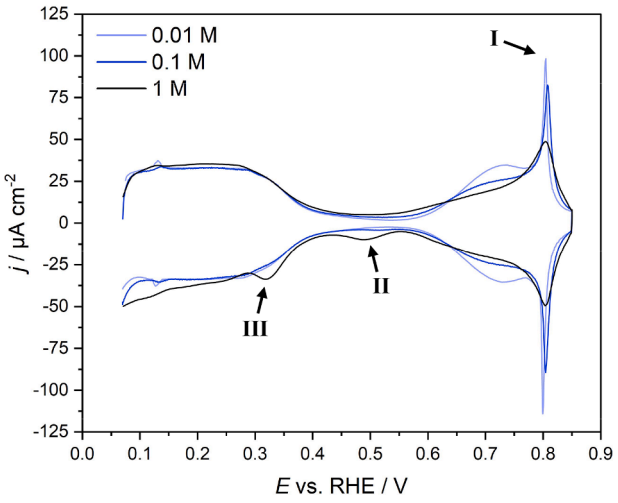

Fig. 1. CV data for Pt(111) as a function of x M aqueous perchloric acid, where $x = 0.01$, 0.1 and 1. Scan rate = 50 mV s^{-1}.

onset potentials of the sharp peak at ~0.8 V (peak I, Fig. 1). These observations are consistent with the results previously reported by Attard et al [31], who attributed this behaviour to the slow catalytic dissociation of specifically adsorbed ClO_4^- onto the Pt surface into Cl^- anions, contributing to a quenching of the charge density with increased concentrations. The subsequent desorption of these Cl^- anions was then argued to result in an electroreduction peak in the double-layer region at 0.45 V. We also observe this electroreduction peak at 0.48 V (peak II, Fig. 1), albeit primarily in 1 M $HClO_4$, as well as an additional reduction peak at 0.32 V (peak III, Fig. 1), both of which will be discussed in more detail later in this manuscript.

The marked attenuation in charge density with increasing concentrations of $HClO_4$, particularly for the OH_{ads} region, indicates the presence of a species that interact with the Pt surface resulting in an observable site-blocking effect [5,31]. In contrast to the work of Attard et al [31], Huang et al [25] argued on the basis of spectroscopic data that this attenuation would be related to the interaction of ClO_4^- anions with the OH adlayer, "specific adsorption" in this context being a perturbation of the OH adlayer that also leads to marked changes in the voltammetric profile.

The appearance of both reduction peaks II and III, as well as the extent of charge density quenching as a function of potential cycling was found to be dependent on the chosen potential window, which, for completely reversible electrochemical processes, should not be the case. Changing the lower vertex potential (LVP) from 0.5 down to 0.06 V in 0.1 V steps revealed that the current density across the CV in both the H_{upd} and OH_{ads} regions could eventually be "recovered", with this recovery occurring quicker with a more negative LVP (SI Fig. 1). In particular, cycling with an LVP of 0.06 V (*i.e.*, the normal potential window for Pt(111) in $HClO_4$), "recovered" the charge density almost entirely across the CV after 30 cycles, showing that cycling regularly into the H_{upd} region expels the accumulated site-blocking species from the surface. This has particular ramifications for experiments in which potentials are held out of the H_{upd} region for long periods of time, such as during microscopy or spectroscopy experiments.

To quantitively elucidate the effect of these site-blocking species on the charge density, 100 potential cycles between 0.3–0.85 V were further carried out in 0.01–1 M $HClO_4$ solutions (Fig. 2). This potential window was chosen as there is no expected oxidation to the Pt single-crystal surface and a lower potential limit of 0.3 V allows the species that results in the reduction peak at 0.32 V (peak III) in 1 M $HClO_4$ to form without cycling too far into the H_{upd} region, such that the charge density is "recovered" as described above (SI Fig. 1). This allows for an explicit assessment of the impact of the presence of the species resulting in reduction peaks II and III comparatively for the different concentrations of $HClO_4$.

As shown in Fig. 2, the current density across both (the onset of) the H_{upd} and OH_{ads} regions significantly decreases with cycling for all 0.01–1 M $HClO_4$ solutions. In particular, the OH_{ads} sharp peak (peak I) becomes markedly quenched as a function of cycling (SI Fig. 2). This effect is less noticeable for 0.01 M (Fig. 2a) as compared to 1 M (Fig. 2c), where the two OH_{ads} regions (*i.e.*, the broader region between ~0.6–0.8 V and the sharp peak I at ~0.8 V) are still distinct for 0.01 M after 100 cycles. By contrast, the two OH_{ads} regions become convoluted under one broad peak in 0.1 M $HClO_4$ after 100 cycles (Fig. 2b), whereas in 1 M $HClO_4$, the OH_{ads} peak becomes very broad and low in intensity after cycling such that the current density has been quenched to the extent that it is now comparable to that in the double-layer region (Fig. 2c). Therefore, the majority of the current density can be attributed to double-layer charging as opposed to pseudocapacitance. By comparison, a relatively substantial pseudocapacitive contribution to the current other than pure double-layer capacitance can still be observed for both 0.01 and 0.1 M $HClO_4$ in the H_{upd} region (0.3–0.4 V) after 100 cycles. This suggests that the quenching of pseudocapacitance increases with $HClO_4$ concentration, pointing to the presence of a species in solution that inhibits the adsorption of H and OH species, the concentration of which is directly correlated to electrolyte concentration.

A corresponding charge density analysis (anodic charge divided by scan rate in the H_{upd} and OH_{ads} regions) (Fig. 3) was carried out on these potential cycling experiments between 0.3–0.85 V to establish this effect more quantitively. These values were then corrected for double-layer charging, *i.e.*, taking the minimum j in the anodic scan in the double-layer region (between 0.4 and 0.6 V) and subtracting across this potential window.

The quenching of the charge density in both the H_{upd}, q_H, measured between 0.3 and 0.4 V (Fig. 3a) and OH_{ads}, q_{OH}, (Fig. 3b) regions becomes much more marked with increasing concentrations of $HClO_4$. After an initial decrease in q_H, a plateau region is reached in both 0.1 and

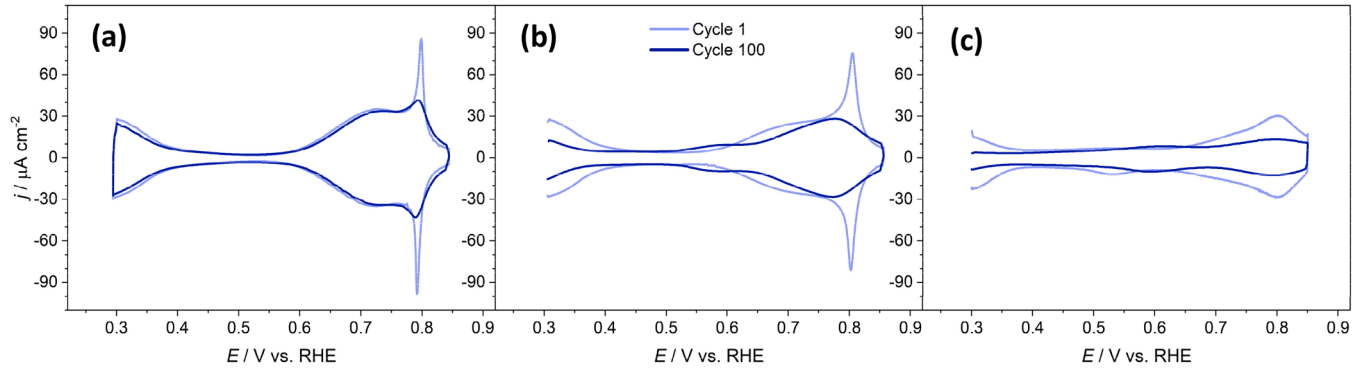

Fig. 2. CVs of cycle 1 and 100 for Pt(111) in (a) 0.01, (b) 0.1, and (c) 1 M $HClO_4$ when carrying out 100 potential cycles between 0.3–0.85 V. Scan rate = 50 mV s^{-1}.

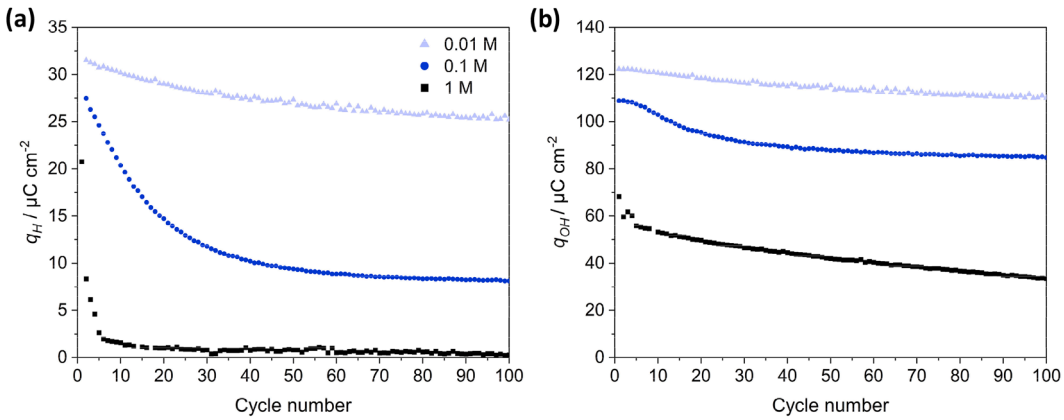

Fig. 3. Charge analysis of Pt(111) for (a) H_{upd} region (0.3–0.4 V) and (b) OH_{ads} region (0.55–0.85 V) *vs.* cycle number in 0.01, 0.1 and 1 M $HClO_4$ with double-layer charge correction obtained from the CVs shown in Fig. 2.

1 M $HClO_4$ within 60 and 5 cycles, respectively. However, in 0.01 M $HClO_4$, this plateau region never seems to be attained within the 100 cycles, indicating that the quenching of q_H is more marked at increasing concentrations of $HClO_4$. The changes in q_{OH} with cycle number for both 0.01 and 0.1 M $HClO_4$ (plateau reached within 40 cycles) show very similar behaviour to that of q_H. By contrast, for 1 M $HClO_4$, after an initial sharp decrease within 5 cycles, q_{OH} continues to decrease with cycle number at a constant rate without reaching a plateau as for q_H. This can be further quantified by correlation plots of q_{OH} *vs.* q_H as a function of $HClO_4$ concentration with cycle number (Fig. 4a), which show clear linear correlations for 0.01 and 0.1 M $HClO_4$. However, for 1 M $HClO_4$, there is some deviation from the linear regime at low cycle numbers, which can be related to the appearance of the electroreduction peak II in the double-layer region at 0.48 V at this concentration, the increased intensity of which mirrors the decrease in q_{OH} with cycling shown with another correlation plot of q_{OH} *vs.* q_{DL} (Fig. 4b).

These results suggest that there is a site-blocking effect caused by a species present in the $HClO_4$ solution itself as both q_H and q_{OH} decrease to a greater extent as a function of increasing electrolyte concentration (assuming negligible pH effects on the RHE scale). This behaviour also discards the accumulation of adsorbed OH as a major cause of site-blocking as this would be expected to show the opposite trend in charge density with increasing $HClO_4$ concentration [21,22].

Specific adsorption of ClO_4^- anions has been argued in the literature to also induce site-blocking effects, which would be consistent with the behaviour we observe in terms of greater quenching of charge density across the CV at higher concentrations of $HClO_4$ [5,46]. Attard et al [31] studied the possibility of this specific adsorption by recording the voltammetric response in 0.1–2 M $HClO_4$ solutions, showing that the sharp peak I at ~0.8 V shifted to more positive onset potentials and became broader with increasing concentration, consistent with our results (Fig. 1). To rule out the attribution of this behaviour to the presence of chaotropic chloride anions in the form of an impurity common in $HClO_4$ [47], micromolar quantities of chloride anions in the form of KCl were introduced into solution resulting in a consequent shift of peak I to more negative onset potentials, opposite to the direction observed when increasing $HClO_4$ concentrations. Instead, Attard et al [31] argued that the site-blocking effect observed with increasing $HClO_4$ concentration was a result of the slow catalytic dissociation of specifically adsorbed ClO_4^- anions to chloride anions, which would then result in the shift in peak I to more positive onset potentials with increasing $HClO_4$ concentrations. However, it should also be noted that they observed the same shift to more positive onset potentials when purposefully spiking $HClO_4$ solutions with micromolar quantities of sulphate [31].

In order to elucidate whether any specific adsorption effects of ClO_4^- were indeed present and to corroborate whether this slow catalytic dissociation to chloride anions could be taking place, we investigated the addition of various quantities of $NaClO_4$ on the voltammetry of Pt (111) in 0.1 M $HClO_4$, as shown in Fig. 5

Additions of $NaClO_4$ to 0.1 M $HClO_4$ cause an increase in the current density of the butterfly peak and a shift to lower onset potentials of peak I (Fig. 5 This behaviour can also be explained partially by an increased affinity for OH adsorption caused by the non-specifically adsorbing Na^+. However, cations have been shown to only minorly affect the OH_{ads} region in acidic media [25,48,49]. Therefore, greater concentrations of ClO_4^- anions up to 0.2 M (0.1 M $HClO_4$ + 0.1 M $NaClO_4$) do not inhibit

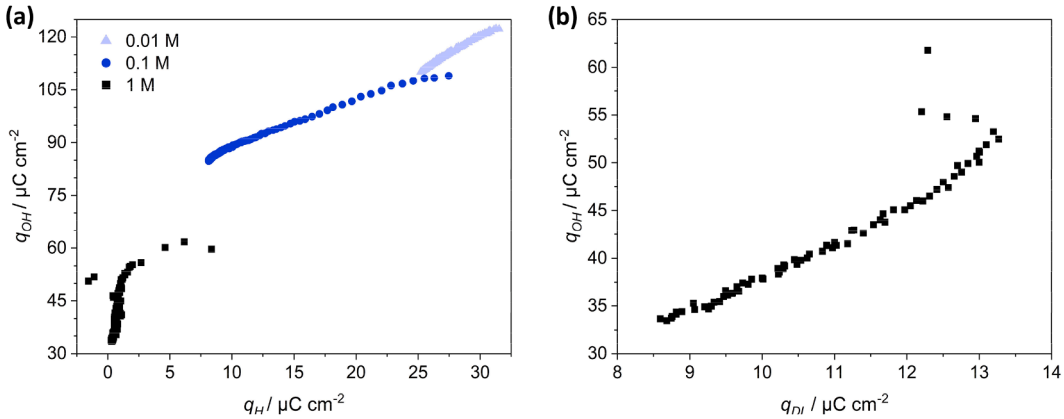

Fig. 4. Correlation plots of (a) q_{OH} *vs.* q_H for 0.01–1 M $HClO_4$ and (b) q_{OH} *vs.* q_{DL} for 1 M $HClO_4$ as a function of cycle number. q_{DL} was taken to be the integral of j between 0.4–0.6 V for the cathodic scan without double-layer charge correction in 1 M $HClO_4$.

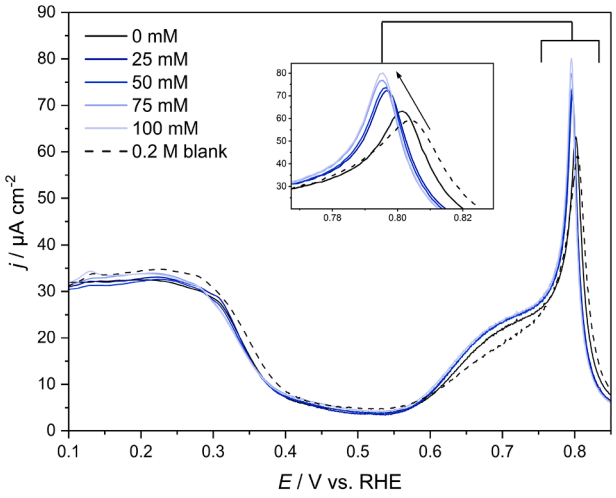

Fig. 5. CV of Pt(111) in 0.1 M $HClO_4$ with various additions of x mM $NaClO_4$, where x = 0, 25, 50, 75 and 100, with blank CV in 0.2 M $HClO_4$ shown for comparison. Scan rate = 50 mV s^{-1}.

the OH_{ads} and H_{upd} charge significantly. By contrast, simply increasing the concentration of $HClO_4$ to 0.2 M results in a non-Nernstian shift of peak I to more positive onset potentials, as well as an attenuation of the charge density. As a reversible hydrogen electrode (RHE) reference was used, pH effects cannot be used to explain this behaviour. We therefore consider that the specific adsorption of ClO_4^- anions is negligibly small for these concentrations.

From the marked changes in the CV of Pt(111) as a function of $HClO_4$ concentrations, it is clear that a species is present in solution that induces site-blocking effects. However, this is unlikely due to the specific adsorption of ClO_4^- anions as indicated by the shift in peak I towards less positive onset potentials with increasing background concentration of ClO_4^- anions. Instead, we show that the effect is likely the result of other impurities that are present even in the high-grade purity $HClO_4$ solutions typically used as electrolytes for Pt single crystal electrochemistry, which would be consistent with the appearance of anomalous reduction peaks at 0.32 (peak III) and 0.48 V (peak II, Fig. 1), as well as the more marked quenching of the charge density across the CV of Pt(111) as a function of increasing concentrations of $HClO_4$ (Fig. 3) [19,31].

Specifically, for both 70 and 60% Merck Suprapur® $HClO_4$, the most abundant impurities are nitrogen and sulphate in 3–10 ppm concentrations (SI Table 1) [50,51]. The specific adsorption of nitrate and sulphate species on Pt surfaces have previously been reported to have a deleterious impact on the charge density of Pt(111) voltammetry via site-blocking [5,46].

In order to mimic the effect of the highest concentration of contaminants present, nitrates and sulfates were introduced in solution in the form of nitric acid and sulphuric acid in 10 ppm concentrations (60 µM), respectively, such that their overall concentration was ~20 ppm in 0.1 M $HClO_4$, *i.e.*, double the amount present in the pure supplied form. The resultant CV is shown in Fig. 6.

As shown in Fig. 6, the additions of HNO_3 and H_2SO_4 resulted in a marked attenuation of peak I, consistent with the presence of competing anions in solution with hydroxyl species for specific adsorption on Pt (111) terrace sites (see SI Fig. 3 for separate addition of 200 µM of HNO_3 to 0.1 M $HClO_4$). Furthermore, the small voltammetric defect (110) peaks in the H_{upd} region are no longer visible, which additionally indicates site-blocking effects in the presence of these species. In particular, upon spiking, two reduction peaks centred at 0.32 V and 0.51 V can be observed, consistent with the peaks III and II, respectively, observed in the blank CV of Pt(111) in 1 M $HClO_4$ (Fig. 1). These could be attributed to nitrate reduction to NO [52,53] and sulphate desorption as the blank Pt(111) CV in 0.1 M H_2SO_4 contains a sharp peak at this potential (SI Fig. 4) [31,54], respectively. Importantly, both reduction peaks II and III are observable in the blank Pt(111)/$HClO_4$ CVs reported in a number of publications, however, with no account of the significance of these peaks [14,44,55–57].

The results in Fig. 6 are also consistent with the work of Feliu et al [58], in which peak II was also found to appear when spiking a 0.1 M $HClO_4$ solution with 2 µM of H_2SO_4. The irreversibility of this peak was discussed to be directly related to the time spent positive of the potential of zero charge (~0.3 V *vs.* NHE [59]), which, in turn, directly affects the amount of adsorbed bisulphate anions.

The reason for the visible asymmetry in the double-layer reduction peak II (*i.e.*, lack of visible oxidation peak) can also be explained by the fact that these contaminants are present in exceedingly low concentrations ($<10^{-4}$M) such that they would be subject to mass-transport limiting effects [5]. In particular, the corresponding oxidation peak is expected to appear at significantly higher potentials, such that the oxidative voltammetric peak would be convoluted under the OH_{ads} oxidation peak in the presence of sulphate anions, *i.e.*, not directly visible in the CV. Indeed, the peak current, i_p, depends linearly on the square-root of the scan rate, v (SI Fig. 5), in accordance with the Randles-Ševčík equation, signifying mass-transport limiting behaviour:

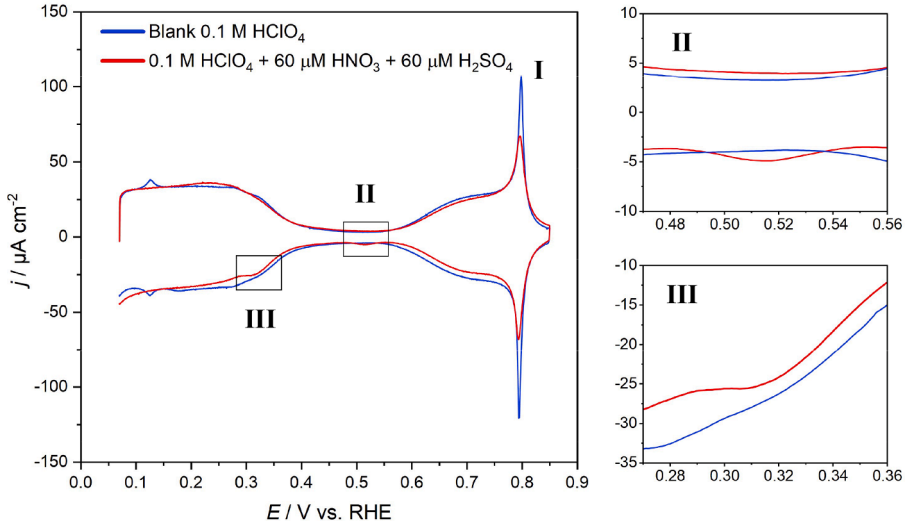

Fig. 6. CV of Pt(111) in 0.1 M $HClO_4$ with 10 ppm (60 µM) additions of HNO_3 and H_2SO_4 with insets showing zoomed-in portions of the graph at which the reduction peaks III and II at 0.32 and 0.51 V appear, respectively. Scan rate = 50 mV s^{-1}.

$$i_p = 0.4463\, n^{3/2}\, F^{3/2}\, A\, \frac{D^{1/2} c\, v^{1/2}}{(RT)^{1/2}} \quad (1)$$

where n is the number of electrons involved; F is Faraday's constant; A is the surface area of the working electrode; D is the diffusion coefficient; c is the redox species' concentration; R is the gas constant; and T is temperature. The OH_{ads} peak (0.55–0.85 V) was also found to have a consistently higher charge for the anodic scan in the OH_{ads} region than for the cathodic scan by 0.4 μC cm^{-2} in 1 M $HClO_4$, which is the same charge (with double-layer correction) under the reduction peak II at 0.5 V, further suggesting that the oxidation peak for the species specifically adsorbed on the Pt(111) is convoluted under this larger OH_{ads} peak, whereas the reduction peak is visible separately.

While the presence of other impurities than sulphate such as chloride and phosphate would also give rise to a reduction peak at similar potentials to peak II, the shift of sharp peak I towards more positive onset potentials with increasing $HClO_4$ concentrations discards chaotropic chloride anions as the major contaminant in this case as this would cause a consequent shift in peak I to more negative onset potentials [5,33]. The observed shift to positive onset potentials in peak I, however, could indeed be consistent with the presence of phosphate anions as both sulphate and phosphate anions are kosmotropic [31,46,60,61]. The higher concentrations of sulphate impurities in the supplied $HClO_4$, however, suggest that this reduction peak is predominantly a result of sulphate desorption.

The reduction peak III centred at 0.32 V was further investigated using *in situ* FTIR spectroscopy and the reduction of nitrate to nitric oxide, NO was confirmed (Fig. 7) [52]. The band that arises at 1650 cm^{-1} has been ascribed to the stretching vibration of on-top N—O and confirms the adsorption of NO on Pt [62]. An increase in the intensity of this band can be observed at potentials included in the H_{upd} region indicating a larger coverage of NO adsorbed on Pt(111) terraces (SI Fig. 6). More importantly, the oxidation of NO at potentials more positive than 0.5 V can be observed and indicates the adsorption of impurities in the double-layer potential window. The reduction peak, however, appears at 0.32 V, indicating that some NO species are likely still present at slightly more positive potentials, *i.e.*, not fully removed from the surface as a function of potential cycling. This same behaviour can be observed in a second band that arises at 2220 cm^{-1} which we tentatively ascribe to the vibration of nitrous oxide (N_2O) [63].

Busó-Rogero et al [64] also observed the appearance of the reduction peaks II and III when using highly concentrated $HClO_4$ solutions (>1 M). In particular, peak III was visible in 3 M $HClO_4$, however, they attributed this reduction peak to the formation of clathrate compounds due to the interaction of H_2O with ClO_4^-. They further investigated these solutions using FTIR spectroscopy and similarly observed a band at 1600–1750 cm^{-1} that increased in intensity with increasing $HClO_4$ concentrations. They attributed this band to the bipolar O—H bending mode of H_2O, discussing that higher $HClO_4$ concentrations introduce more H-bonding inhibition as a function of cycling due to the interaction of perchlorate anions with interfacial water and subsequent clathrate formation. However, given that reduction peak III is highly irreversible in nature and our previous discussion of the negligible specific adsorption of perchlorate anions, it is unlikely that the sole reason for this behaviour are the formation of these clathrate compounds, particularly for the concentrations of $HClO_4$ we have investigated. Instead, we suggest that it is more likely that this behaviour can be attributed to the presence of nitrate trace impurities.

Unfortunately, resolution below 1400 cm^{-1}, where the sulphate stretching frequency would be observed was not sufficient with our FTIR spectroscopy setup, so we were not able to detect sulphate adsorption directly [65]. However, given that the reduction of nitrates to NO species has been detected using *in situ* FTIR spectroscopy and sulphates are present in the same range of concentrations in the supplied $HClO_4$ (SI Table 1), peak II is most likely attributable to sulphates.

In this FTIR configuration, only a thin layer of electrolyte is present between the electrode surface and the prism such that mass transport of species in the electrolyte becomes restricted. In this sense, we have focused the discussion of this manuscript on the qualitative detection of NO species in the electrolyte, as opposed to a direct quantitative analysis. We also assume that pH effects are negligible as an RHE reference electrode has been used, however, this assumption could be challenged due to restricted proton transport in this thin-layer configuration. In order to validate this assumption, we carried out CVs before and after FTIR measurements, both of which showed no potential shifts.

It should be noted that the presence of chloride anions has been

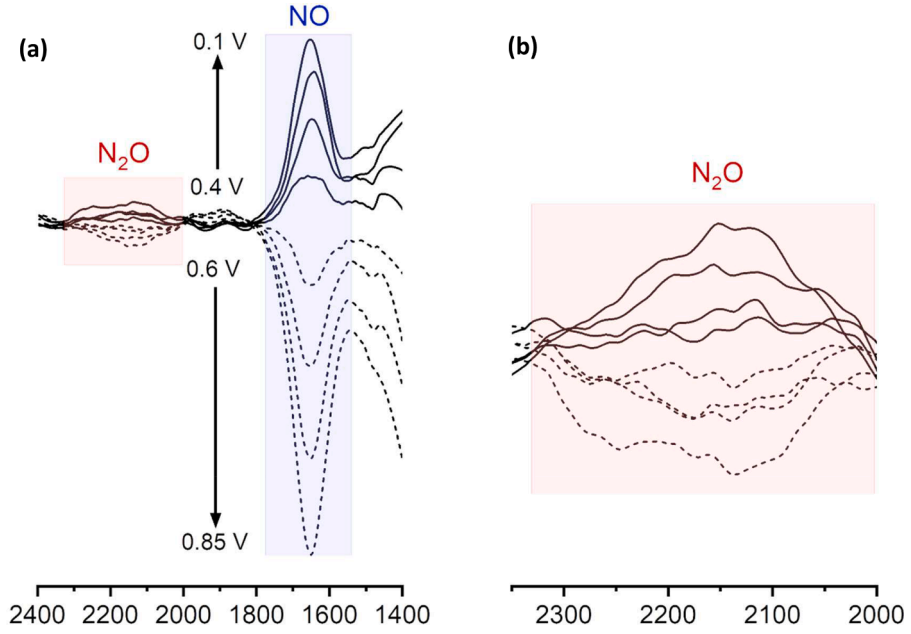

Fig. 7. (a) In situ FTIR spectra as a function of potential of Pt(111) in 0.1 M $HClO_4$ with bands corresponding to on-top N—O (blue) and N_2O (red) vibrations. (b) Inset zoomed-in on second band between 2000–2300 cm^{-1}. The reference spectrum was collected at 0.5 V and the sample spectra were acquired every 10 mV. (For interpretation of the references to color in this figure legend, the reader is referred to the web version of this article.)

shown to have no inhibitive effect on the H_{upd} charge, and neither should sulphate impurities [66]. Instead, the inhibition of q_H is likely to be a result of the nitrate/NO species present. The inhibitive site-blocking nature of these impurities for OH_{ads} also has potentially severe ramifications for the efficiency of electrocatalytic processes such as the oxygen reduction reaction (ORR), as well as more fundamental studies in which it is often assumed that electrolyte effects are negligible in the case of perchloric acid.

4. Conclusion

The presence of trace impurities in high-grade purity aqueous perchloric acid solutions is non-negligible, its effect on the cyclic voltammetry of Pt(111) depending on the used electrolyte concentration and applied scan rate. In particular, we showed that marked attenuations are seen in the charge density across the CV of Pt(111) with $HClO_4$ concentrations up to 1 M that we attribute to a site-blocking effect from nitrate and sulphate impurities.

While a shift of the OH_{ads} butterfly peak towards more positive potentials corresponding to site blocking effect of Pt active sites is observed for 0.2 M $HClO_4$, the shift towards more negative onset potentials observed at 0.1 M $HClO_4$ + 0.1 M $NaClO_4$ rejects the slow catalytic dissociation of specifically adsorbed ClO_4^- as a possible cause for the loss in charge density. However, the possibility of an interaction of ClO_4^- anions with the OH adlayer causing the marked changes in the Pt(111) CV as a function of potential cycling cannot be discarded, extending the meaning of the term "specific adsorption" to influencing the adsorption of other chemisorbates.

Using *in situ* FTIR spectroscopy, we detected the reduction of nitrate species to NO even in low concentration 0.1 M $HClO_4$, further detectable by the appearance of a reduction peak in the CV of Pt(111) centred at 0.32 V. We suggest that the mass-transport limited electroreduction peak in the double-layer region centred at ~0.5 V arises from the specific adsorption of sulphate, also present in low concentrations in $HClO_4$ high-purity solutions. Given the high affinity of Pt for both nitrate/nitric oxide and sulphate, the marked attenuations seen as a function of increasing $HClO_4$ concentrations across the CV of Pt(111) and, by extension, other single crystal surfaces, can be attributed at least partially to the presence of these contaminants. This renders the assumption that $HClO_4$ contains only non-specifically adsorbing species invalid under certain conditions.

In particular, the presence of both nitrates and sulphates becomes problematic at high concentrations of $HClO_4$ (>1 M). As shown, these impurities also contribute to a quenching of the charge density across the CV of Pt(111) if the H_{upd} potential region is avoided for too long, which has significant ramifications for *in situ* spectroscopy and/or microscopy techniques where applied potentials are held for long periods of time outside of the H_{upd} window.

While the observations reported here are not all new, we believe that we have collected here sufficient evidence in a single paper to clearly outline the conditions under which one must be careful with excluding the effect of trace impurities, and what their precise origin is. As a result, we suggest the following measures in order to limit the effect of these contaminants in $HClO_4$ electrolyte for Pt(111) and, by extension, other Pt single crystal studies:

1. Avoid using high concentration $HClO_4$ solutions (>1 M).
2. Cycle regularly into the H_{upd} region.
3. Remove trace level impurities through previously reported purification methods [42].
4. Avoid using a slow scan rate (< 10 mV s^{-1}).

CRediT authorship contribution statement

Nicci Fröhlich: Investigation, Methodology, Data curation, Conceptualization, Formal analysis, Visualization, Writing – original draft, Writing – review & editing. **Julia Fernández-Vidal:** Investigation, Methodology, Data curation, Formal analysis, Visualization, Writing – review & editing, Writing – original draft, Writing – review & editing. **Francesc Valls Mascaró:** Conceptualization, Investigation, Validation, Writing – review & editing. **Arthur J. Shih:** Conceptualization, Validation, Writing – review & editing. **Mingchuan Luo:** Conceptualization, Writing – review & editing. **Marc T.M. Koper:** Funding acquisition, Conceptualization, Formal analysis, Supervision, Resources, Project administration, Writing – review & editing.

Declaration of Competing Interest

The authors declare that they have no known competing financial interests or personal relationships that could have appeared to influence the work reported in this paper.

Data availability

Data will be made available on request.

Acknowledgements

This work received funding from the European Research Council (ERC), Advanced Grant No. 101019998 "FRUMKIN", as well as being part of the research programme TOP with project number 716.017.001, which is financed by The Netherlands Organisation for Scientific Research (NWO). Funding was also received from the Innovation Framework Programme (Marie Skłodowska-Curie actions Individual Fellowship awarded to M.L., No. 897818). JFV also gratefully acknowledges Dr. Amanda C. Garcia for receiving FTIR spectroscopy training.

Supplementary materials

Supplementary material associated with this article can be found, in the online version, at doi:10.1016/j.electacta.2023.143035.

References

[1] J. Clavilier, A. Rodes, K.El Achi, M.A Zamakhchari, Electrochemistry at platinum single crystal surfaces in acidic media : hydrogen and oxygen adsorption, J. Chim. Phys. 88 (1991) 1291–1337.
[2] J. Clavilier, The role of anion on the electrochemical behaviour of a {111} platinum surface; an unusual splitting of the voltammogram in the hydrogen region, J. Electroanal. Chem. Interfac. Electrochem. 107 (1980) 211–216.
[3] G.A. Attard, A. Ahmadi, D.J. Jenkins, O.A. Hazzazi, P.B. Wells, K.G. Griffin, P. Johnston, J.E. Gillies, The characterisation of supported platinum nanoparticles on carbon used for enantioselective hydrogenation: a combined electrochemical–STM approach, ChemPhysChem 4 (2003) 123–130.
[4] R.M. Arán-Ais, M.C. Figueiredo, F.J. Vidal-Iglesias, V. Climent, E. Herrero, J. M. Feliu, On the behavior of the Pt(100) and vicinal surfaces in alkaline media, Electrochim. Acta 58 (2011) 184–192.
[5] A. Berná, V. Climent, J.M Feliu, New understanding of the nature of OH adsorption on Pt(111) electrodes, Electrochem. Commun. 9 (2007) 2789–2794.
[6] H. Kita, S. Ye, A. Aramata, N. Furuya, Adsorption of hydrogen on platinum single crystal electrodes in acid and alkali solutions, J. Electroanal. Chem. Interfacial Electrochem. 295 (1990) 317–331.
[7] A.J. Bard, L.R. Faulkner, E.lectrochemical Methods: Fundamentals and Application, John Wiley & Sons, Inc., 2000.
[8] R. Rizo, E. Herrero, V. Climent, J.M. Feliu, On the nature of adsorbed species on Platinum Single Crystal electrodes, Curr. Opin. Electrochem. 38 (2023), 101240.
[9] J.J. Calvante, N.S. Marinković, Z. Kováčová, W. Ronald Fawcett, SNIFTIRS studies of the double layer at the metal/solution interface. Part 1. Single crystal gold electrodes in aqueous perchloric acid, J. Electroanal. Chem. 421 (1997) 49–57.
[10] R. Rizo, R.M. Arán-Ais, E. Herrero, On the oxidation mechanism of C1-C2 organic molecules on platinum. A comparative analysis, Curr. Opin. Electrochem. 25 (2021), 100648.
[11] C. Korzeniewski, V. Climent, J. Feliu, Electrochemistry At Platinum Single Crystal Electrodes in Electroanalytical Chemistry A Series of Advances, CRC Press, 2011. *Volume 24*.
[12] M.D. Pohl, V. Colic, D. Scieszka, A.S. Bandarenka, Elucidation of adsorption processes at the surface of Pt(331) model electrocatalysts in acidic aqueous media, Phys. Chem. Chem. Phys. 18 (2016) 10792–10799.

[13] K.A. Jaaf-Golze, D.M. Kolb, D. Scherson, On the voltammetry of curves of Pt (111) in aqueous solutions, J. Electroanal. Chem. Interfacial Electrochem. 200 (1986) 353–362.
[14] J. Clavilier, R. Albalat, R. Gomez, J.M. Orts, J.M. Feliu, A. Aldaz, Study of the charge displacement at constant potential during CO adsorption on Pt(110) and Pt (111) electrodes in contact with a perchloric acid solution, J. Electroanal. Chem. 330 (1992) 489–497.
[15] M.D. Maciá, J.M. Campiña, E. Herrero, J.M. Feliu, On the kinetics of oxygen reduction on platinum stepped surfaces in acidic media, J. Electroanal. Chem. 564 (2004) 141–150.
[16] M.J. Kolb, F. Calle-Vallejo, L.B.F. Juurlink, M.T.M Koper, Density functional theory study of adsorption of H2O, H, O, and OH on stepped platinum surfaces, J. Chem. Phys. 140 (2014), 134708.
[17] J. Clavilier, R. Faure, G. Guinet, R. Durand, Preparation of monocrystalline Pt microelectrodes and electrochemical study of the plane surfaces cut in the direction of the {111} and {110} planes, J. Electroanal. Chem. Interfac. Electrochem. 107 (1980) 205–209.
[18] I. Takahashi, S.S. Kocha, Examination of the activity and durability of PEMFC catalysts in liquid electrolytes, J. Power Sources 195 (2010) 6312–6322.
[19] K. Shinozaki, J.W. Zack, R.M. Richards, B.S. Pivovar, S.S. Kocha, Oxygen reduction reaction measurements on platinum electrocatalysts utilizing rotating disk electrode technique: I. Impact of impurities, measurement protocols and applied corrections, J. Electrochem. Soc. 162 (2015) F1144.
[20] M.T.M. Koper, Blank voltammetry of hexagonal surfaces of Pt-group metal electrodes: comparison to density functional theory calculations and ultra-high vacuum experiments on water dissociation, Electrochim. Acta 56 (2011) 10645–10651.
[21] V. Climent, J.M. Feliu, Thirty years of platinum single crystal electrochemistry, J. Solid State Electrochem. 15 (2011) 1297–1315.
[22] R. Rizo, J. Fernández-Vidal, L.J. Hardwick, G.A. Attard, F.J. Vidal-Iglesias, V. Climent, E. Herrero, J.M. Feliu, Investigating the presence of adsorbed species on Pt steps at low potentials, Nat. Commun. 13 (2022) 2550.
[23] J. Chen, S. Luo, Y. Liu, S. Chen, Theoretical analysis of electrochemical formation and phase transition of oxygenated adsorbates on Pt(111), ACS Appl. Mater. Interfaces 8 (2016) 20448–20458.
[24] M.T.M. Koper, J.J. Lukkien, Modeling the butterfly: the voltammetry of $(\sqrt{3}\times\sqrt{3})R30^{\circ}$ and p(2×2) overlayers on (111) electrodes, J. Electroanal. Chem. 485 (2000) 161–165.
[25] Y.-F. Huang, P.J. Kooyman, M.T.M Koper, Intermediate stages of electrochemical oxidation of single-crystalline platinum revealed by *in situ* Raman spectroscopy, Nat. Commun. 7 (2016) 12440.
[26] A.M. Gómez-Marín, R. Rizo, J.M. Feliu, Some reflections on the understanding of the oxygen reduction reaction at Pt(111), Beilstein J. Nanotechnol. 4 (2013) 956–967.
[27] A.S. Bondarenko, I.E.L. Stephens, H.A. Hansen, F.J. Pérez-Alonso, V. Tripkovic, T. P. Johansson, J. Rossmeisl, J.K. Nørskov, I. Chorkendorff, The Pt(111)/electrolyte interface under oxygen reduction reaction conditions: an electrochemical impedance spectroscopy study, Langmuir 27 (2011) 2058–2066.
[28] A.S. Bandarenka, H.A. Hansen, J. Rossmeisl, I.E.L. Stephens, Elucidating the activity of stepped Pt single crystals for oxygen reduction, Phys. Chem. Chem. Phys. 16 (2014) 13625–13629.
[29] J. Solla-Gullón, P. Rodríguez, E. Herrero, A. Aldaz, J.M. Feliu, Surface characterization of platinum electrodes, Phys. Chem. Chem. Phys. 10 (2008) 1359–1373.
[30] M.T.M. Koper, J.J. Lukkien, N.P. Lebedeva, J.M. Feliu, R.A. van Santen, Adsorbate interactions and phase transitions at the stepped platinum/electrolyte interface: experiment compared with Monte Carlo simulations, Surf. Sci. 478 (2001) L339–L344.
[31] G.A. Attard, A. Brew, K. Hunter, J. Sharman, E. Wright, Specific adsorption of perchlorate anions on Pt{hkl} single crystal electrodes, Phys. Chem. Chem. Phys. 16 (2014) 13689–13698.
[32] A.P. Sandoval, M.F. Suárez-Herrera, V. Climent, J.M. Feliu, Interaction of water with methanesulfonic acid on Pt single crystal electrodes, Electrochem. Commun. 50 (2015) 47–50.
[33] B. Hribar, N.T. Southall, V. Vlachy, K.A. Dill, How ions affect the structure of water, J. Am. Chem. Soc. 124 (2002) 12302–12311.
[34] A.H.B. Dourado, Electric double layer: the good, the bad, and the beauty, Electrochem 3 (2022) 789–808. Preprint at.
[35] K. Kunimatsu, H. Hanawa, H. Uchida, M. Watanabe, Role of adsorbed species in methanol oxidation on Pt studied by ATR-FTIRAS combined with linear potential sweep voltammetry, J. Electroanal. Chem. 632 (2009) 109–119.
[36] H. Uchida, H. Ozuka, M. Watanabe, Electrochemical quartz crystal microbalance analysis of CO-tolerance at Pt-Fe alloy electrodes, Electrochim. Acta 47 (2002) 3629–3636.
[37] D.V. Tripkovic, D. Strmcnik, D. van der Vliet, V. Stamenkovic, N.M. Markovic, The role of anions in surface electrochemistry, Farad. Discuss. 140 (2009) 25–40.
[38] N. Li, J. Lipkowski, Chronocoulometric studies of chloride adsorption at the Pt (111) electrode surface, J. Electroanal. Chem. 491 (2000) 95–102.
[39] S.P. Liu, M. Zhao, W. Gao, T. Jacob, Q. Jiang, Nature of the electrochemical HClO4/Pt(111) interface, Appl. Surf. Sci. 400 (2017) 426–433.
[40] T.J. Schmidt, U.A. Paulus, H.A. Gasteiger, R.J. Behm, The oxygen reduction reaction on a Pt/carbon fuel cell catalyst in the presence of chloride anions, J. Electroanal. Chem. 508 (2001) 41–47.
[41] D. Strmcnik, D. Li, P.P. Lopes, D. Tripkovic, K. Kodama, V.R. Stamenkovic, N. M. Markovic, When small is big: the role of impurities in electrocatalysis, Top. Catal. 58 (2015) 1174–1180.
[42] D. Strmcnik, V. Stamenkovic, N. Markovic, Electrochemical Filter for Removal of Trace Level Ions, 2019.
[43] B. Garlyyev, S. Xue, M.D. Pohl, D. Reinisch, A.S. Bandarenka, Oxygen electroreduction at high-index Pt electrodes in alkaline electrolytes: a decisive role of the alkali metal cations, ACS Omega 3 (2018) 15325–15331.
[44] A. Kolics, A. Wieckowski, Adsorption of bisulfate and sulfate anions on a Pt(111) electrode, J. Phys. Chem. B 105 (2001) 2588–2595.
[45] T. Iwasita, F.C. Nart, In-situ Fourier transform infrared spectroscopy: a tool to characterize the metal-electrolyte interface at a molecular level. Advances in Electrochemical Science and Engineering, Wiley Blackwell, 2008, pp. 123–216, vol. 4.
[46] J. Mostany, P. Martínez, V. Climent, E. Herrero, J.M. Feliu, Thermodynamic studies of phosphate adsorption on Pt(111) electrode surfaces in perchloric acid solutions, Electrochim. Acta 54 (2009) 5836–5843.
[47] M. Arenz, V. Stamenkovic, T.J. Schmidt, K. Wandelt, P.N. Ross, N.M. Markovic, The effect of specific chloride adsorption on the electrochemical behavior of ultrathin Pd films deposited on Pt(111) in acid solution, Surf. Sci. 523 (2003) 199–209.
[48] M. Nakamura, Y. Nakajima, N. Hoshi, H. Tajiri, O. Sakata, Effect of non-specifically adsorbed ions on the surface oxidation of Pt(111), ChemPhysChem 14 (2013) 2426–2431.
[49] D. Strmcnik, K. Kodama, D. van der Vliet, J. Greeley, V.R. Stamenkovic, N. M. Marković, The role of non-covalent interactions in electrocatalytic fuel-cell reactions on platinum, Nat. Chem. 1 (2009) 466–472.
[50] Merck, Perchloric Acid 60% for Analysis EMSURE® ACS Specification Sheet, 2020, 1.00518.2501.
[51] Merck, Perchloric Acid 70% Suprapur® Specification Sheet, 2018, 1.00517.0250.
[52] G.E. Dima, G.L. Beltramo, M.T.M Koper, Nitrate reduction on single-crystal platinum electrodes, Electrochim. Acta 50 (2005) 4318–4326.
[53] E.B. Molodkina, I.G. Botryakova, A.V. Rudnev, M.R Ehrenburg, Redox-transitions in NO/NH_3 adlayers on a Pt(111) electrode in an acidic solution, Electrochim. Acta 444 (2023), 141997.
[54] A.M. Funtikov, U. Stimming, R. Vogel, Anion adsorption from sulfuric acid solutions on Pt(111) single crystal electrodes, J. Electroanal. Chem. 428 (1997) 147–153.
[55] T. Kondo, T. Masuda, N. Aoki, K. Uosaki, Potential-dependent structures and potential-induced structure changes at Pt(111) single-crystal electrode/sulfuric and perchloric acid interfaces in the potential region between hydrogen underpotential deposition and surface oxide formation by in situ surface X-Ray scattering, J. Phys. Chem. C 120 (2016) 16118–16131.
[56] E. Sibert, R. Faure, R. Durand, High frequency impedance measurements on Pt (111) in sulphuric and perchloric acids, J. Electroanal. Chem. 515 (2001) 71–81.
[57] G. García, M.T.M Koper, Stripping voltammetry of carbon monoxide oxidation on stepped platinum single-crystal electrodes in alkaline solution, Phys. Chem. Chem. Phys. 10 (2008) 3802–3811.
[58] J.M. Feliu, R. Gómez, M.J. Llorca, A. Aldaz, Electrochemical behavior of irreversibly adsorbed selenium dosed from solution on Pt(h,k,l) single crystal electrodes in sulphuric and perchloric acid media, Surf. Sci. 289 (1993) 152–162.
[59] R. Rizo, E. Sitta, E. Herrero, V. Climent, J.M. Feliu, Towards the understanding of the interfacial pH scale at Pt(111) electrodes, Electrochim. Acta 162 (2015) 138–145.
[60] I.Y. Zhang, G. Zwaschka, Z. Wang, M. Wolf, R.K. Campen, Y. Tong, Resolving the chemical identity of H_2SO_4 derived anions on Pt(111) electrodes: they're sulfate, Phys. Chem. Chem. Phys. 21 (2019) 19147–19152.
[61] Z. Su, V. Climent, J. Leitch, V. Zamlynny, J.M. Feliu, J. Lipkowski, Quantitative SNIFTIRS studies of (bi)sulfate adsorption at the Pt(111) electrode surface, Phys. Chem. Chem. Phys. 12 (2010) 15231–15239.
[62] K. Nakata, A. Okubo, K. Shimazu, A. Yamakata, S. Ye, M. Osawa, Surface-enhanced infrared absorption spectroscopic studies of adsorbed nitrate, nitric oxide, and related compounds 1: reduction of adsorbed no on a platinum electrode, Langmuir 24 (2008) 4352–4357.
[63] G. Socrates, Infrared and Raman Characteristic Group Frequencies: Tables and Charts, Wiley, 2004.
[64] C. Busó-Rogero, A. Ferre-Vilaplana, E. Herrero, J.M. Feliu, The role of formic acid/formate equilibria in the oxidation of formic acid on Pt (111), Electrochem. Commun. 98 (2019) 10–14.
[65] F.C. Nart, T. Iwasita, M. Weber, Vibrational spectroscopy of adsorbed sulfate on Pt (111), Electrochim. Acta 39 (1994) 961–968.
[66] N. Garcia-Araez, V. Climent, E. Herrero, J. Feliu, J. Lipkowski, Thermodynamic studies of chloride adsorption at the Pt(111) electrode surface from 0.1M HClO4 solution, J. Electroanal. Chem. 576 (2005) 33–41.